

CO₂ capture using aqueous 1-(2-Hydroxyethyl) piperidine and its blends with piperazine: Solubility and enthalpy

Shubhashis Adak, Madhusree Kundu*

Department of Chemical Engineering, National Institute of Technology, Rourkela, India

ARTICLE INFO

Article history:

Received 4 August 2019

Received in revised form

3 January 2020

Accepted 6 January 2020

Available online 13 January 2020

Keywords:

CO₂ capture

1-(2-Hydroxyethyl) piperidine

Piperazine

Activity coefficient model

pKa

Enthalpy

ABSTRACT

In this article, equilibrium CO₂ solubility in aqueous 1-(2-Hydroxyethyl) piperidine (HEP) solutions pertaining concentrations (1, 2, 3) mol/L in the temperature range (303.15–323.15) K, and CO₂ partial pressure range 0.1–100 kPa are presented. HEP, being a tertiary alkanolamine, its rate of CO₂ absorption is comparatively slower than primary or secondary alkanolamine. Piperazine (PZ), a rate promoter was added to HEP in 1:4 mol ratio to form blends having enhance rate of CO₂ absorption. Equilibrium CO₂ solubility in four different aqueous blends; (0.8 mol/L HEP + 0.2 mol/L PZ), (1.6 mol/L HEP + 0.4 mol/L PZ), (2.4 mol/L HEP + 0.6 mol/L PZ), (3.2 mol/L HEP + 0.8 mol/L PZ) were measured over the temperature range of (303.15–323.15) K and CO₂ partial pressure spanning over 0–70 kPa. Equilibrium constant for deprotonation reaction of HEP was estimated by measuring pKa of aqueous HEP solution at 298.15, 303.15, 313.15, 323.15 and 333.15 K. Experimentally obtained CO₂ solubility data for single and blended amine solutions were correlated efficiently using activity coefficient model with AAD % of 3.76 and 3.22, respectively. Speciation of both single and blended amine solutions in their equilibrated liquid phase were predicted. Interaction parameters obtained through thermodynamic modelling of equilibrium solubility data for single and blended amine solutions were used to predict the enthalpy of CO₂ absorption.

© 2020 Elsevier B.V. All rights reserved.

1. Introduction

Sustainable development of technology is a dire need of the present time. In the prevailing state of technology, huge quantity of CO₂ is being thrown from thermal power plant, natural gas purification installations, steel industry and refineries. There is a need to control Carbon dioxide emission from various point sources by revamping the current technology to its benign form. For CO₂ appropriation, chemical absorption using amine based solvents is the most mature and suitable technology till date. Major obstacle before this technology is high energy requirement for solvent regeneration. Energy requirement for solvent regeneration varies depending upon the nature of the solvent. In case of primary or secondary alkanolamines, energy requirement for solvent regeneration is high compared to tertiary alkanolamines. Because for the former cases, CO₂ gets absorbed through the formation of highly stable carbamate ion whereas bicarbonate formation takes place in case of tertiary alkanolamines. On the other hand, rate of CO₂

absorption for primary and secondary alkanolamine is higher than tertiary alkanolamine, however tertiary alkanolamine possess higher CO₂ absorption capacity compared to primary or secondary alkanolamine. Solvent selection plays vital role in chemical absorption process. To make this process economic, solvents should possess high CO₂ absorption capacity and rate and lower regeneration energy. One can formulate solvent blends having optimal characteristics suitable for chemical absorption process. Researches across the Globe have taken focussed R&D initiatives regarding the formulation of various aqueous blended solvents for chemical absorption of CO₂. Among these solvent blends, aqueous piperazine (PZ) promoted N-methyldiethanolamine (MDEA) blend acquired lot of attentions (Xu et al. [1], Liu et al. [2], Kamps et al. [3], Bottinger et al. [4], Speyer et al. [5], Derks et al. [6], Svensson et al. [7], and Huang et al. [8]). Equilibrium CO₂ solubility in aqueous PZ promoted 2-Diethylaminoethanol (DEAE) blend was generated and correlated using Kent Eisenberg model [9]. Ramezani et al. [10] studied CO₂ absorption capacity, absorption rate and corrosion rate for five blends consisting of trisodium phosphate (TSP) as base solvent and 2-((2-aminoethyl) amino) ethanol (AEEA), methyl-diethanolamine (MDEA), piperazine (PZ), potassium sarcosinate (K-

* Corresponding author.

E-mail address: mkundu@nitrrkl.ac.in (M. Kundu).

Sar) and potassium lysinate (K-Lys) as additives. They concluded that highest CO₂ absorption rate, highest CO₂ absorption capacity, and highest corrosion rate were manifested by (TSP + PZ), (TSP + K-Lys), and (TSP + PZ) blends, respectively. Du and Rochelle [11] have screened 36 aqueous PZ based amine blends based on their thermal degradation, amine volatility, CO₂ cyclic capacity, and CO₂ absorption rate for CO₂ capture from flue gas. Diverse amine structures including imidazoles, cyclic and long-chain diamines, tertiary amines, hindered amines, hindered and tertiary amino acids, and ether amines were selected to formulate blends with PZ. They found that 2.5 m PZ/2.5 m amine blends react faster with CO₂ than 7 m monoethanolamine (MEA) solution. It is to be noted that CO₂ loading expressed by them is different than many others in the relevant contemporary literature including us. Chowdhury et al. [12] selected twenty four tertiary alkanolamines as CO₂ absorbent and they found seven promising compounds which perform better than industrially used N-Methyldiethanolamine (MDEA) in terms of absorption capacity, absorption rate and cyclic capacity for CO₂. Among these seven tertiary alkanolamines, 1-(2-Hydroxyethyl) piperidine (HEP) possesses some excellent properties to be regarded as a novel CO₂ absorbent. Xiao et al. [13] carried out VLE experiments in aqueous HEP solution at different temperature and CO₂ pressure. HEP, being a tertiary alkanolamine, its rate of CO₂ absorption is comparatively slower than MEA. Piperazine, a secondary cyclic diamine is very attractive compound for its high CO₂ absorption rate as well as capacity, however due to the formation of very stable carbamate; it demands high regeneration energy [14]. PZ can be used to promote the rate of absorption in blends with HEP. Hence, (HEP + PZ) blend is likely to possess promising properties of a novel CO₂ absorbent. Apart from rate, VLE of CO₂ in HEP and its blend with PZ, thermodynamic modelling, speciation, enthalpy of CO₂ absorption, studies on corrosion and foaming properties should be carried out to promote this solvent formulation suitable for CO₂ absorption. In view of this, equilibrium solubility data in aqueous HEP and its PZ promoted blends were generated at different conditions and solubility data were correlated using activity coefficient model. From the activity coefficient model liquid phase concentration of different species present at equilibrium have been estimated. Heat of absorption of CO₂ is of primary concern for CO₂ capture process because regeneration energy is the prime factor in screening solvent, hence, feasibility of this process. Enthalpy of solution due to CO₂ absorption in both aqueous HEP and its PZ promoted blends were predicted.

2. Experimental section

2.1. Materials

HEP, PZ, MDEA, MEA, CO₂ were used for the experimentation. The structure of the compounds, their purity along with their sources is presented in Table 1. Millipore water (Merck Millipore, (Milli-Q)) having conductivity value of $1 \times 10^{-7} \Omega^{-1} \text{ cm}^{-1}$ and surface tension 72 mN.m⁻¹ at 298 K was used for solution preparation. Distilled water was degassed by boiling, then it was cooled to ambient temperature under vacuum and used for making the amine solutions. Uncertainty in volumetric measurement was $\pm 0.057 \text{ cm}^3$. Composition of aqueous HEP and [HEP + PZ] blends used in this study in molarity (mol/L) or equivalent molality (mol/kg H₂O) unit are presented in Table 2.

2.2. Measurement of pKa

The equilibrium constant for deprotonation reaction of HEP was estimated by measuring pKa of the solution over the temperature range of (298.15–333.15) K by potentiometric titration. Detailed

experimental method for pKa measurement was discussed in our earlier published work [9] and same method is adopted in this study for pKa measurement.

2.3. Vapour-liquid equilibrium measurement

2.3.1. Experimental set-up

The equilibrium CO₂ solubility in aqueous HEP and (HEP + PZ) blends were measured in stainless steel made equilibrium stirred cell reactor. The same VLE set-up was utilised for the solubility measurements as well as screening experiment which was used in our previous work [9].

2.4. Experimental method of CO₂ solubility

Present experimental set-up utilised two vessels namely buffer and equilibrium vessels. The vessels were made to reach the temperature of the constant temperature water bath (maintained using recirculation temperature controller, Polyscience, USA model No: 9712) with an uncertainty in temperature by $\pm 0.05 \text{ K}$. Both the vessels (buffer and the equilibrium) were evacuated concurrently using vacuum pump (HINDVAC). After evacuation, the buffer vessel got insulated from equilibrium vessel. The buffer vessel is capable of handling a total pressure of 1.5–2.5 times to that of the desired maximum CO₂ partial pressure or total pressure attained by the equilibrium vessel and it is being filled up using pure CO₂ gas cylinder. 25 ml of freshly prepared amine solution (single or blended amine) with specific composition was put into the equilibrium vessel. Afterwards, the equilibrium vessel was evacuated for the second time and rested under solution vapour pressure (p_v). The solution vapour pressure was recorded. The maximum error expected in the volume dispatched is estimated to be 0.05 ml. The CO₂ gas from the buffer vessel was transferred to the equilibrium vessel. During the absorption process in the equilibrium vessel, the buffer vessel was disconnected from the equilibrium vessel. The moles of CO₂ dispatched from the buffer vessel was estimated using the final and initial pressure reading of the pressure transducer (Swagelok, model No: PTI-S-NA-100-15AO-B) attached to the buffer vessel ($u(P_1) = 0.031 \text{ kPa}$). During the absorption, liquid phase in the equilibrium vessel went on stirring by magnetic stirrer (SPINOT). The observed time to reach equilibrium varies depending upon the solution. The pressure transducer fitted to the equilibrium vessel (Swagelok, model No: PTI-S-NA-50-15AO-B, $u(P_2) = 0.021 \text{ kPa}$) showed the total vessel pressure (P_t). The equilibrium CO₂ partial pressure (P_{CO_2}) was estimated to be the difference of the total equilibrium vessel pressure (P_t) and solution vapour pressure (p_v). The moles of CO₂ absorbed by the amine solution was estimated using moles of CO₂ being dispatched from the buffer vessel and the moles of CO₂ present in the vapour space of the equilibrium vessel at a specific equilibrium pressure (compressibility factor of the gas was considered in CO₂ mole calculations as described by Park and Sandall [15]). CO₂ loading is expressed as moles of CO₂ absorbed per moles of solvent at a specific equilibrium CO₂ pressure and temperature. Successive runs at a specific temperature can be taken by repeating the whole procedure already stated. It is to be noted that successive readings on CO₂ solubility was taken at still higher CO₂ pressures than the previous ones because of the diminishing capacity of the solution. The experimental procedure for the VLE measurement using this set-up was validated in our previously published work [9].

2.5. Background of solvent selection

The same VLE set-up as mentioned earlier was used to carry out the screening experiment. Solvent screening was carried out

Table 1
Chemicals used in this work along with their structure, purity and sources.

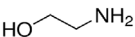
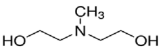
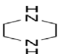
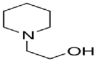
Compound	Structure	Purity	Supplier
Monoethanolamine (MEA)		≥99 (mol %)	Sigma Aldrich
Methyldiethanolamine (MDEA)		≥99 (mol %)	Sigma Aldrich
Piperazine (PZ)		≥99 (mol %)	Merck
1-(2-Hydroxyethyl)piperidine (HEP)		≥99 (mol %)	Merck
Carbon Dioxide (CO ₂)	O=C=O	99.9 (mol %)	Vadilal Gases Limited

Table 2
Composition of aqueous HEP and (HEP + PZ) blends in molarity (mol/L) and equivalent molality (mol/kg) unit.

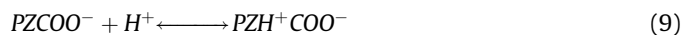
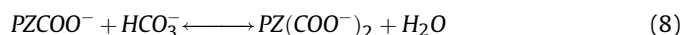
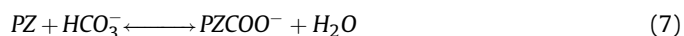
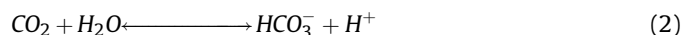
HEP		HEP + PZ	
Molarity (mol/L)	Molality (mol/kg)	Molarity (mol/L)	Molality (mol/kg)
1	1.149	0.8 + 0.2	0.92 + 0.23
2	2.689	1.6 + 0.4	2.12 + 0.53
3	4.878	2.4 + 0.6	3.76 + 0.94
		3.2 + 0.8	6.20 + 1.55

qualitatively by comparing the CO₂ loading (g-CO₂/L-solution) with respect to time (1000 s span). For this screening experiment MEA, MDEA, HEP, PZ and (MDEA + PZ), (HEP + PZ) blends were chosen. All the experiments were carried out at 313.15 K. 25 ml of the 1 (mol/L) freshly prepared aqueous amine solution was taken in the previously evacuated equilibrium cell and specific amount of CO₂ was transferred from the buffer cell to the equilibrium cell. The pressure drop in the equilibrium cell due to CO₂ absorption was recorded using NI data acquisition card (NI USB 6008) for 1000 s time span. Pressure difference in the buffer cell (before and after CO transfer) was noted for further calculation. CO₂ loading (g-CO₂/L-solution) was calculated as discussed in the previous subsection. CO₂ loading data of each of the aforesaid absorbents was presented in Figs. 1 and 2 to compare their CO₂ absorption capacity within a specific time span.

From, Fig. 1, it was found that HEP performs better than MDEA in terms of absorption capacity and apparent rate of CO₂ absorption but having relatively slower rate of absorption in comparison to MEA. PZ manifested the highest CO₂ absorption capacity and rate among the single amines under consideration. Hence, PZ was used as rate promoter in (MDEA + PZ) and (HEP + PZ) blends. PZ was added in the blends in (PZ: MDEA/HEP = 1:4) a specific ratio. From Fig. 2, it has been found that (0.8 mol/L HEP + 0.2 mol/L PZ) blend possess very close apparent rate and comparatively high absorption capacity in comparison to 1 mol/L MEA. On the other hand, (0.8 mol/L HEP + 0.2 mol/L PZ) blend reveals higher apparent rate and absorption capacity in comparison to (0.8 mol/L MDEA + 0.2 mol/L PZ) blend. As the apparent rate of PZ is very high, addition of PZ in the blend in a higher ratio is expected to increase the apparent rate of the blend. However, PZ forms very stable carbamate while reacting with CO₂. Thus, during thermal regeneration process same amount of energy must be supplied to break the bond. On the other hand, HEP carbamate formation is not possible due to presence of bulky groups at amine-nitrogen and CO₂ is solely absorbed by the formation of bicarbonate ion. Hence, for VLE measurements in different (HEP + PZ) blends, HEP: PZ ratio was maintained at 4:1.

2.6. Model development

Chemical Equilibria: When CO₂ reacts with aqueous single HEP solution, the following reactions take place as per eqs. (1)–(4) and in case of reaction of CO₂ with (HEP + PZ) blend, reactions occur according to eqs. (1)–(9).



The equilibrium constants (K_1 – K_9) for these above reactions are expressed as:

$$K_1 = \frac{[H^+][OH^-]}{[H_2O]} \quad (10)$$

$$K_2 = \frac{[HCO_3^-][H^+]}{[CO_2]} \frac{\gamma_{HCO_3^-} \gamma_{H^+}}{\gamma_{CO_2}} \quad (11)$$

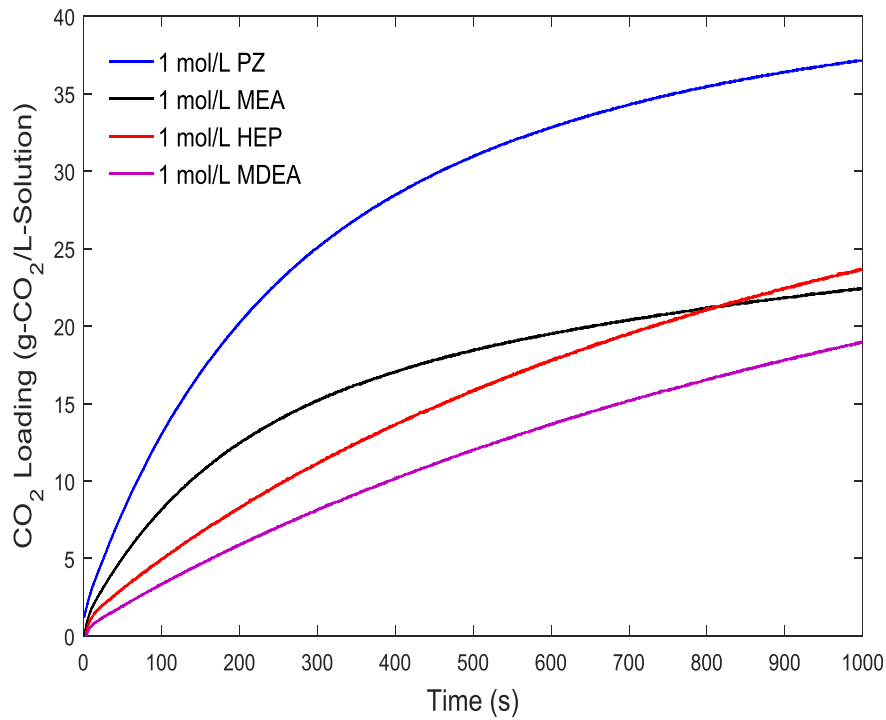


Fig. 1. Apparent rate of CO₂ absorption in 1 mol/L PZ, MEA, HEP and MDEA at 313.15 K.

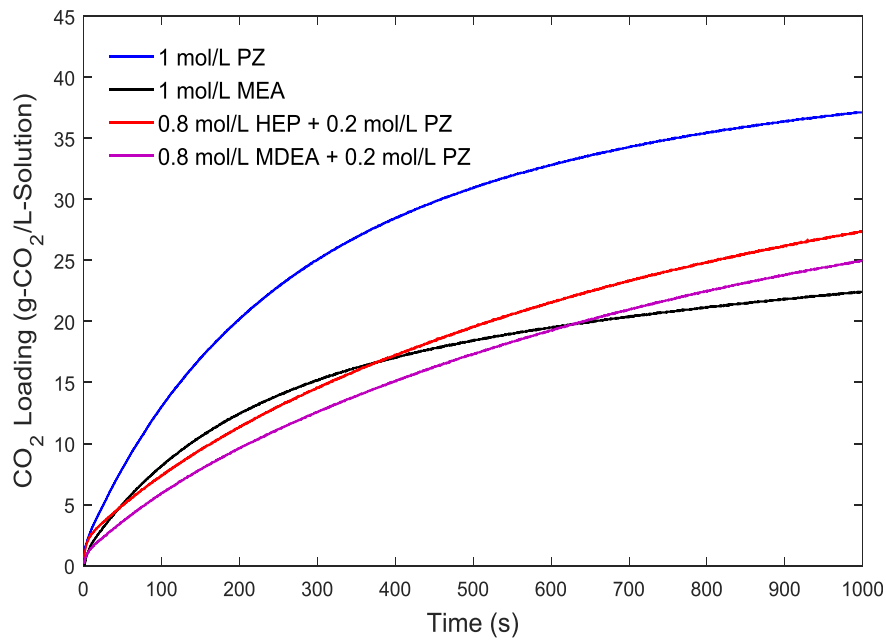


Fig. 2. Apparent rate of CO₂ absorption in 1 mol/L PZ, MEA and PZ promoted HEP and MDEA blends at 313.15 K.

$$K_3 = \frac{[CO_3^{2-}][H^+]}{[HCO_3^-]} \frac{\gamma_{CO_3^{2-}} \gamma_{H^+}}{\gamma_{HCO_3^-}} \quad (12)$$

$$K_4 = \frac{[HEPH^+]}{[HEP][H^+]} \frac{\gamma_{HEPH^+}}{\gamma_{HEP} \gamma_{H^+}} \quad (13)$$

$$K_5 = \frac{[PZH^+]}{[PZ][H^+]} \frac{\gamma_{PZH^+}}{\gamma_{PZ} \gamma_{H^+}} \quad (14)$$

$$K_6 = \frac{[PZH_2^{2+}]}{[PZH^+][H^+]} \frac{\gamma_{PZH_2^{2+}}}{\gamma_{PZH^+} \gamma_{H^+}} \quad (15)$$

$$K_7 = \frac{[PZCOO^-][H_2O]}{[PZ][HCO_3^-]} \frac{\gamma_{PZCOO^-} \gamma_{H_2O}}{\gamma_{PZ} \gamma_{HCO_3^-}} \quad (16)$$

$$K_8 = \frac{[PZ(COO^-)_2][H_2O]}{[PZCOO^-][HCO_3^-]} \frac{\gamma_{PZ(COO^-)_2} \gamma_{H_2O}}{\gamma_{PZCOO^-} \gamma_{HCO_3^-}} \quad (17)$$

$$K_9 = \frac{[PZH^+COO^-]}{[PZCOO^-][H^+]} \frac{\gamma_{PZH^+COO^-}}{\gamma_{PZCOO^-} \gamma_{H^+}} \quad (18)$$

where $[i]$ and γ_i are the concentration and activity coefficient of the i th species, respectively. The temperature dependency of the equilibrium constants as well as Henry's constant are expressed as:

$$K_i / H_{CO_2} = \exp\left(\frac{a_i}{T} + b_i \ln T + c_i T + d_i\right) \quad (19)$$

For the reactions (1–9), all the parameters (a_i to d_i) are taken from literature [16–18]; except K_4 and are presented in Table 3. In addition to the above equations, the following set of conditions must also be satisfied.

For single aqueous HEP solution

Charge balance for **single aqueous HEP solution**:

$$H^+ + HEPH^+ = OH^- + HCO_3^- + 2CO_3^{2-} \quad (20)$$

CO₂ balance:

$$\alpha[HEP]_{total} = HCO_3^- + CO_3^{2-} + CO_2 \quad (21)$$

HEP balance:

$$[HEP]_{total} = HEP + HEPH^+ \quad (22)$$

where α is the CO₂ loading.

For aqueous (HEP + PZ) blend solution.

Charge balance for **aqueous (HEP + PZ) blend solution**:

$$HEPH^+ + PZH^+ + 2 * PZH_2^{2+} + H^+ = PZCOO^- + 2 * PZ(COO^-)_2 + HCO_3^- + 2CO_3^{2-} + OH^- \quad (23)$$

CO₂ balance:

$$\alpha([HEP]_{total} + [PZ]_{total}) = PZCOO^- + 2 * PZ(COO^-)_2 + HCO_3^- + CO_3^{2-} + CO_2 \quad (24)$$

HEP balance:

$$[HEP]_{total} = HEP + HEPH^+ \quad (25)$$

PZ balance:

$$[PZ]_{total} = PZ + PZH^+ + PZH_2^{2+} + PZCOO^- + 2 * PZ(COO^-)_2 + PZH^+COO^- \quad (26)$$

The concentration of CO₂ in the liquid phase can be estimated by Henry's law:

$$\phi_{CO_2} P_{CO_2} = \gamma_{CO_2} H_{CO_2} [CO_2] \quad (27)$$

P_{CO_2} is partial pressure of CO₂, ϕ_{CO_2} is the fugacity coefficient of gas phase, H_{CO_2} is the Henry's constant. In this study, gas phase non ideality was not considered.

For single aqueous HEP solutions, set of nonlinear equations (10)–(13) and (20)–(22) and (27) were solved simultaneously to find out a 5th order nonlinear equation in terms of H^+ ion concentration present in the liquid phase considering liquid phase activity coefficient as 1.

For aqueous (HEP + PZ) blend solutions, set of nonlinear equations (2) and (10)–(18) 3–27 were solved simultaneously and a 8th order nonlinear equation in terms of H^+ ion concentration was obtained considering activity coefficient of different species present in the liquid phase as 1.

Later, Non-ideality of the liquid phase was considered by calculating activity coefficients of different species present in the solution using modified Debye-Huckel theory for the electrolytic solution [19].

$$\ln \gamma_i = -\frac{AZ_i^2 \sqrt{I}}{1 + B\sqrt{I}} + 2 \sum_j \beta_{ij} m_j \quad (28)$$

A is temperature dependent Debye-Huckel constant and B is taken as 1.2 [20]. m_j and Z_i are concentration and electrical charge of the i th species. I is the ionic strength of the solution and is calculated as:

$$I = \frac{1}{2} \sum_j m_j Z_j^2 \quad (29)$$

β_{ij} is binary interaction parameter between different molecular and ionic species present in the liquid phase.

A large number of interactions are possible between the species present in solution but some of them have negligible effect on activity coefficient. Species having high concentration have larger influence on activity coefficient than species present in very low concentration. Also interaction between species of same ionic charge was neglected. In this study, total 17 binary interaction parameters for single amine solution and total 34 binary interaction parameters for (HEP + PZ) blend were considered to develop the activity coefficient models.

Interaction parameters were obtained by regressing the experimental solubility data at different temperatures and amine concentrations. In this study, the interaction parameters were estimated by minimizing the objective function

$$F = (1/N) \sum_{i=1}^N \left[\frac{(\alpha_{i,exp} - \alpha_{i,cal})}{\alpha_{i,exp}} \right]^2 * 100 \quad (31)$$

where N is the total number of measurements taken during experiment, $\alpha_{i,exp}$ is the experimental CO₂ loading and $\alpha_{i,cal}$ is the calculated CO₂ loading. Total 64 and 157 experimentally obtained data points were used for the regression of binary interaction

Table 3

Parameters used for the estimation of equilibrium constant (molality scale) and Henry's constant (atm.kg/mol) in activity coefficient model.

Parameter	a_i	b_i	c_i	d_i	Source
K_1	−13445.9	−22.4773	0	140.932	[16]
K_2	−12092.1	−36.7816	0	235.482	[16]
K_3	−12431.7	−35.4819	0	220.067	[16]
$1/K_4$	−2.6651	17.4615	0	−121.7606	This work
K_5	3814.4	0	−0.015096	14.119	[17]
K_6	2192.3	0	−0.017396	10.113	[17]
K_7	3616.1	0	0	−8.635	[18]
K_8	1322.3	0	0	−3.655	[18]
K_9	3493.1	0	0	10.026	[18]
HCO_2	−6789.04	−11.4519	−0.010454	94.4914	[18]

parameter in single and blended amine solutions, respectively.

2.7. Enthalpy prediction from CO₂ solubility data

When CO₂ reacts with aqueous HEP and (HEP + PZ) blended solutions, number of chemical reactions occur. All the reactions are associated with some energy change. The combination of heat of reaction of CO₂ with amine and heat of dissolution is the heat of absorption of CO₂ in solvents.

Enthalpy of CO₂ absorption can be predicted using interaction parameters obtained from regression of equilibrium CO₂ solubility data. Overall enthalpy is the sum of enthalpy associated with every single reaction (chemical and physical). Enthalpy of reaction, Q_i (KJ) for every single reaction can be calculated from eqn. (32).

$$Q_i = \epsilon_i \left(\Delta H_i^0 + \sum_j \nu_{j,i} H_j^E \right) \quad (32)$$

ΔH_i^0 is the standard reaction enthalpy, H_j^E is the partial excess molar enthalpy of species j , $\nu_{j,i}$ is the stoichiometric coefficient of species j and ϵ_i is the extent of reaction.

Standard enthalpy of reaction, ΔH_i^0 and partial excess molar enthalpy, H_j^E can be calculated using van't Hoff equation (33) and equation (34) respectively.

$$\Delta H_i^0 = RT^2 \left(\frac{\partial \ln K_i}{\partial T} \right)_p \quad (33)$$

$$H_j^E = -RT^2 \left(\frac{\partial \ln \gamma_j}{\partial T} \right) \quad (34)$$

Enthalpy of absorption due to physical dissolution of CO₂, ΔH_{phy} was calculated using equation (35).

$$\Delta H_{phy} = -RT^2 \left(\frac{\partial \ln H_{CO_2}}{\partial T} \right) + RT^2 \left(\frac{\partial \ln \gamma_{CO_2}}{\partial T} \right) \quad (35)$$

Overall enthalpy of solution, ΔH_{sol} (KJ/mol of CO₂) due to CO₂ absorption in the amine solution was calculated using equation (36).

$$\Delta H_{sol} = \Delta H_{phy} + \frac{1}{n_{CO_2}} \sum_i Q_i \quad (36)$$

n_{CO_2} is the mole of CO₂ absorbed at equilibrium.

3. Results and discussions

3.1. pKa of HEP

Method of pKa measurements was validated by measuring the same for MDEA in the temperature range of (298.15–333.15) K (revealed an AAD% of 0.91 in comparison to the data available in the open literature) [9]. Experimentally obtained pKa data of HEP in the temperature range (298.15–333.15) K are presented in Table 4. Xu et al. [21] measured the pKa of HEP in the temperature range of (288.15–333.15) K. Experimental pKa data obtained in this work has been compared with the literature data in Fig. 3. From Fig. 3, it is evident that pKa measured in this work is very close with the literature data. pKa values in the said temperature range were used for estimating the deprotonation constant of HEP, which was useful in the development of activity coefficient model using experimentally measured CO₂ solubility data in aqueous HEP and (HEP + PZ) blends.

Table 4

Experimentally obtained pKa values of HEP in the temperature range (298.15–333.15) K.

Temperature (K)	pKa
303.15	9.524
313.15	9.358
323.15	9.078
333.15	8.831

$$u(ph) = \pm 0.032, \quad u(t) = \pm 0.05K, \quad \%AAD = |((pKa_{exp} - pKa_a) / pKa_{exp})| * 100$$

3.2. VLE of [CO₂ (1) + HEP (2) + H₂O (3)] system

VLE of (CO₂ (1) + HEP (2) + H₂O (3)) system was measured in the HEP concentration range of (1, 2, 3) mol/L, at temperatures (303.15, 313.15, and 323.15) K and in the pressure range (0–100) kPa. CO₂ solubility are presented in Tables S1–S3 (supplementary file).

All the experimental CO₂ solubility data (64 data) were correlated using thermodynamically sound activity coefficient model. Experimental and model predicted data are compared as shown in Fig. 4a–c. To calculate the activity coefficient of individual species present in the liquid phase, total 17 interaction parameters were considered. Interactions between same ionic charge species were neglected and species having very low concentration (H⁺, OH[−], CO₃^{2−}) were also neglected. Developed model ensures excellent agreement between the experimental and model predicted loading having average absolute deviation percentage (AAD %) of 2.76. Interaction parameters obtained by regression of experimental data using the thermodynamic model are presented in Table 5. These interaction parameters were further used to predict the enthalpy of absorption of the (CO₂ (1) + HEP (2) + H₂O (3)) system.

The experimental pH values obtained by Xiao et al. [6] with respect to CO₂ loading at 1(M) HEP and 303.15 K are compared with the model estimated pH value (present work) at same experimental condition and results are presented in Fig. 5. Some pH values were predicted corresponding to extrapolated loading data below our experimental loading (0.42) and one pH value was interpolated. Model predicted pH corresponding to our experimental range are in excellent agreement with the experimental pH data obtained by Xiao et al. [13] and little deviations are seen in case of extrapolated data, which is below our experimental range. These results substantiate the efficiency of the developed activity coefficient model; as well as authenticity of experimental solubility data generated.

3.3. VLE of [CO₂ (1) + HEP (2) + PZ (3) + H₂O (4)] system

VLE of (CO₂ (1) + HEP (2) + PZ (3) + H₂O (4)) systems were measured at temperature (303.15, 313.15, 323.15) K and pressure range of (0–70) KPa. Four different aqueous blends, [0.8 mol/L HEP + 0.2 mol/L PZ], [1.6 mol/L HEP + 0.4 mol/L PZ], [2.4 mol/L HEP + 0.6 mol/L PZ], [3.2 mol/L HEP + 0.8 mol/L PZ] were used for VLE measurements at above mentioned temperatures and pressure range. Experimentally obtained CO₂ solubility data are presented in Tables S4–S7 (supplementary file). Experiments were carried out at different temperatures, amine compositions and CO₂ partial pressures to study the effect of temperature, concentration and pressure on CO₂ loading. As expected, it has been found that CO₂ loading decreases with increasing temperature and amine concentration and increases with increasing CO₂ partial pressure.

All these experimental CO₂ solubility data (157 data) were used to develop an activity coefficient model which could correlate the experimental data at different experimental conditions. Being blends, a large number of species (HEP, HEPH⁺, PZ, PZH⁺, PZH₂²⁺, PZCOO[−], PZ (COO[−])₂, PZH⁺COO[−], HCO₃[−], CO₃^{2−}, CO₂, H⁺, OH[−]) are

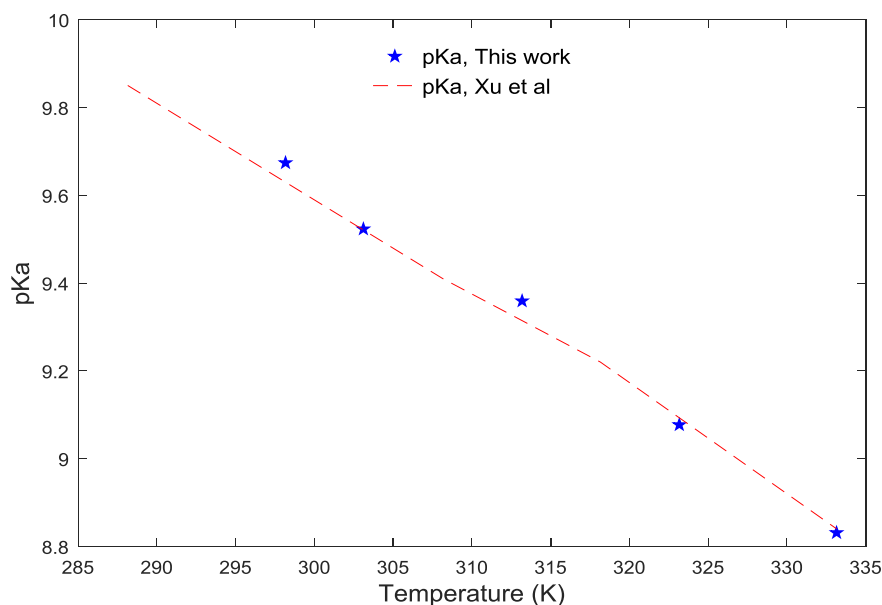


Fig. 3. Comparison of experimental pKa of HEP measured in this work and pKa measured by Xu et al. at different temperatures.

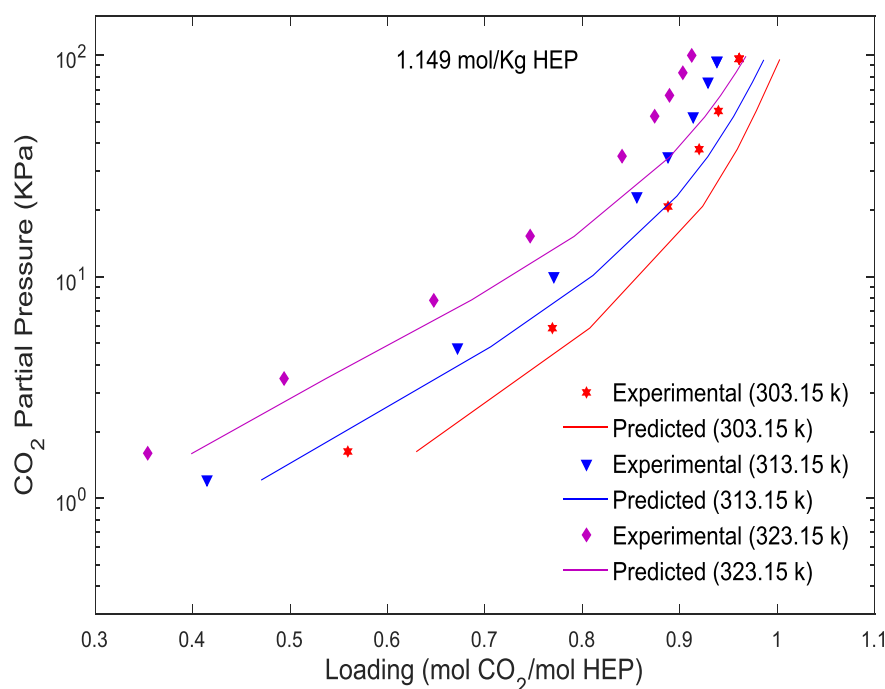


Fig. 4a. Equilibrium solubility in (CO₂ (1) + HEP (2) + H₂O (3)): Experimental and model predicted CO₂ loading for (1.149 mol HEP/kg H₂O) at 303.15, 313.15 and 323.15 K.

formed when they react with CO₂. Hence, quite a large number of interactions among species are possible. We have considered only interactions of the types namely, cation-anion, cation-molecule, anion-molecule, molecule-molecule. Interactions between cation-cation and anion-anion were neglected. Interactions between species with very low concentration (H⁺, OH⁻, CO₃²⁻) were also neglected. Protonated piperazine carbamate (PZH⁺COO⁻) was considered as a molecule with net ionic charge zero. Total 34 interaction parameters were considered for development of activity coefficient model and optimized interaction parameters are presented in Table 6.

Developed activity coefficient model can correlate experimental

loading at different experimental condition (temperature, blend composition, CO₂ partial pressure) with an AAD% of 3.22. The developed model predicts loading very efficiently, which is very much evident from Fig. 6a–d. For [1.6 mol/L HEP + 0.4 mol/L PZ], [2.4 mol/L HEP + 0.6 mol/L PZ] and [3.2 mol/L HEP + 0.8 mol/L PZ] systems, model predicted loadings are very close to experimentally measured loading. However, for [0.8 mol/L HEP + 0.2 mol/L PZ] system, deviation between predicted and experimental loading is little high at 313.15 and 323.15 K. All the interaction parameters obtained by regression of solubility data were further used to calculate enthalpy of CO₂ absorption for different blends at three different temperatures.

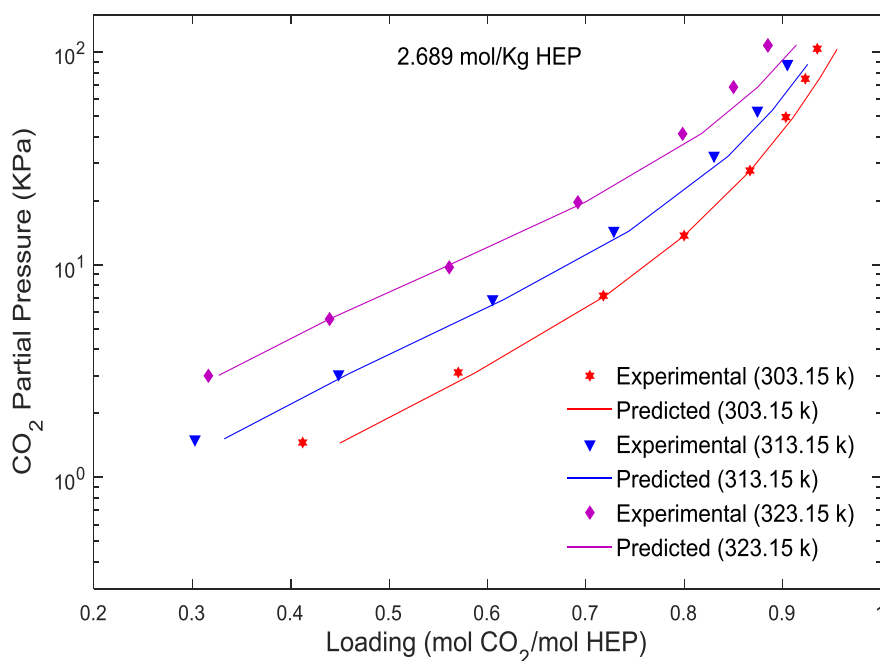


Fig. 4b. Equilibrium solubility in (CO_2 (1) + HEP (2) + H_2O (3)): Experimental and model predicted CO_2 loading for (2.689 mol HEP/kg H_2O) at 303.15, 313.15 and 323.15 K.

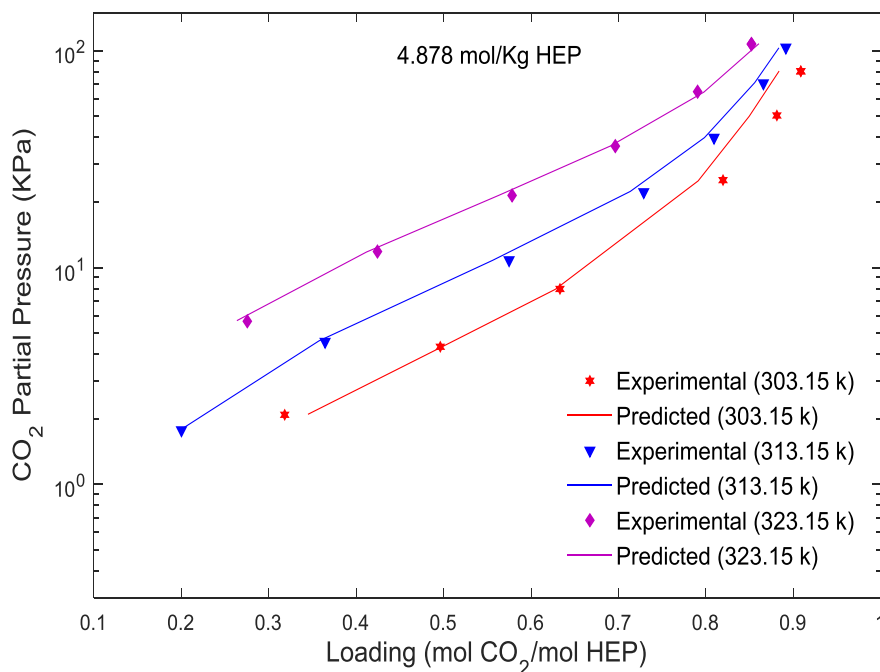


Fig. 4c. Equilibrium solubility in (CO_2 (1) + HEP (2) + H_2O (3)): Experimental and model predicted CO_2 loading for (4.878 mol HEP/kg H_2O) at 303.15, 313.15 and 323.15 K.

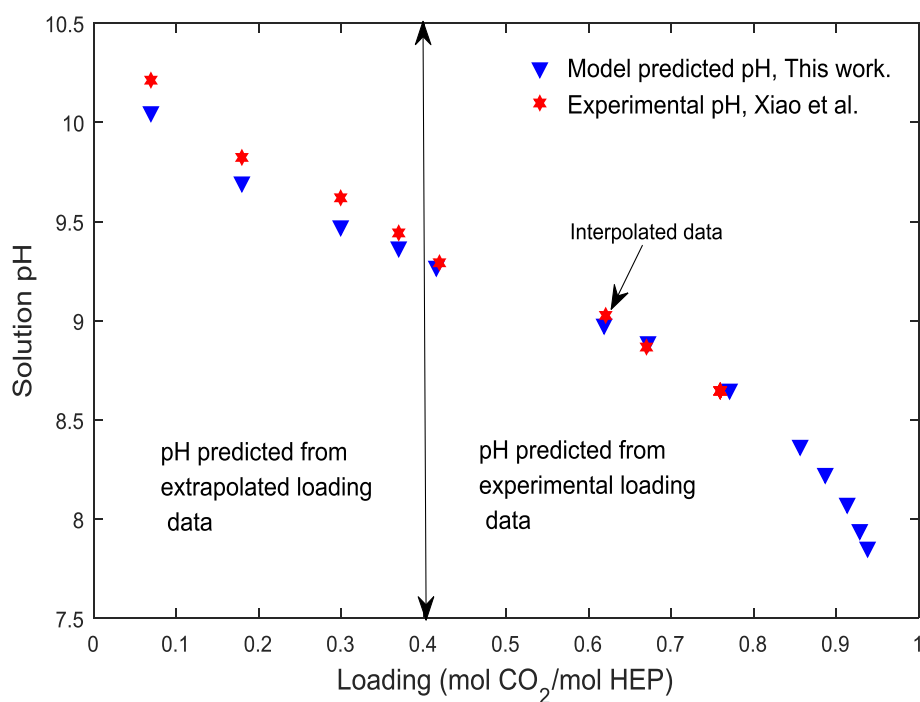
3.4. Speciation of [CO_2 (1) + HEP (2) + H_2O (3)] system

When CO_2 reacts with HEP, different species are formed and concentration of each species changes with progression of the reaction. The species concentrations at equilibrated liquid phase were calculated from the thermodynamic model. Concentrations of different species present in the solution changes with respect to loading according to Fig. 7. With increasing loading, concentration of HEP decreases gradually because of protonation reaction and consequently concentration of protonated HEP (HEPH^+) increases

gradually. Being tertiary in nature, HEP carbamate formation is not possible due to presence of three bulky groups at amine group and CO_2 is solely absorbed by the formation of bicarbonate ion (HCO_3^-). Hence, concentration of bicarbonate ion increases gradually with respect to loading. Concentration of carbonate ion (CO_3^{2-}) initially increases and reaches maximum at loading of 0.5 and then decreases gradually. This phenomenon can be explained by the fact that, initially at loading close to zero the concentration of HEP is very high consequently the pH of the solution is very high (close to 10). In this situation some free HEP molecules act like a base and

Table 5Optimized binary interaction parameters obtained from activity coefficient model of equilibrium CO₂ solubility data in aqueous HEP solution.

Parameters	Optimized Value (kg/mol)	Parameters	Optimized Value (kg/mol)
$\beta_{\text{CO}_2-\text{H}^+}$	0.069475	$\beta_{\text{H}^+-\text{HEP}}$	0.027641
$\beta_{\text{CO}_2-\text{HEPH}^+}$	-0.2405	$\beta_{\text{HEPH}^+-\text{OH}^-}$	0.074034
$\beta_{\text{CO}_2-\text{OH}^-}$	0.068151	$\beta_{\text{HEPH}^+-\text{HCO}_3^-}$	0.181132
$\beta_{\text{CO}_2-\text{HCO}_3^-}$	0.312331	$\beta_{\text{HEPH}^+-\text{CO}_3^{2-}}$	0.210693
$\beta_{\text{CO}_2-\text{CO}_3^{2-}}$	-0.20255	$\beta_{\text{OH}^+-\text{HEP}}$	0.374511
$\beta_{\text{CO}_2-\text{HEP}}$	0.098617	$\beta_{\text{HCO}_3^--\text{HEP}}$	0.025661
$\beta_{\text{H}^+-\text{OH}^-}$	0.082661	$\beta_{\text{CO}_3^{2-}-\text{HEP}}$	0.013871
$\beta_{\text{H}^+-\text{HCO}_3^-}$	0.029099	$\beta_{\text{CO}_2-\text{H}^+}$	0.269743
$\beta_{\text{H}^+-\text{CO}_3^{2-}}$	0.057658		

**Fig. 5.** Comparison of experimental and model predicted solution pH with CO₂ loading in 1 mol/L HEP solution at 313.15 K.**Table 6**Optimized binary interaction parameters obtained from activity coefficient model of equilibrium CO₂ solubility data in aqueous (HEP + PZ) solution.

Parameters	Optimized Value (kg/mol)	Parameters	Optimized Value (kg/mol)
$\beta_{\text{CO}_2-\text{HEPH}^+}$	-0.17684	$\beta_{\text{HEP}-\text{PZCOO}^-}$	-0.09159
$\beta_{\text{CO}_2-\text{PZCOO}^-}$	-0.15748	$\beta_{\text{HEP}-\text{PZ}(\text{COO}^-)_2}$	0.686586
$\beta_{\text{CO}_2-\text{PZ}(\text{COO}^-)_2}$	0.657523	$\beta_{\text{HEP}-\text{HCO}_3^-}$	-0.03347
$\beta_{\text{CO}_2-\text{HCO}_3^-}$	0.162158	$\beta_{\text{HEP}-\text{CO}_3^{2-}}$	0.167437
$\beta_{\text{CO}_2-\text{PZH}^+}$	-0.03693	$\beta_{\text{PZ}-\text{CO}_2}$	0.04539
$\beta_{\text{HEPH}^+-\text{PZCOO}^-}$	0.698306	$\beta_{\text{PZ}-\text{HEPH}^+}$	-0.12902
$\beta_{\text{HEPH}^+-\text{PZ}(\text{COO}^-)_2}$	0.751241	$\beta_{\text{PZ}-\text{PZCOO}^-}$	-0.04051
$\beta_{\text{HEPH}^+-\text{HCO}_3^-}$	0.031848	$\beta_{\text{PZ}-\text{PZ}(\text{COO}^-)_2}$	-0.01489
$\beta_{\text{PZCOO}^-}-\text{PZH}^+$	0.236741	$\beta_{\text{PZ}-\text{HCO}_3^-}$	0.670032
$\beta_{\text{PZ}(\text{COO}^-)_2}-\text{PZH}^+$	0.208451	$\beta_{\text{PZ}-\text{PZH}^+}$	0.299113
$\beta_{\text{PZH}^+-\text{COO}^-}-\text{HEPH}^+$	0.495796	$\beta_{\text{PZH}_2^+-\text{CO}_2}$	0.300579
$\beta_{\text{PZH}^+-\text{COO}^-}-\text{PZCOO}^-$	0.27479	$\beta_{\text{PZH}_2^+-\text{PZCOO}^-}$	0.293847
$\beta_{\text{PZH}^+-\text{COO}^-}-\text{PZ}(\text{COO}^-)_2$	0.109209	$\beta_{\text{PZH}_2^+-\text{PZ}(\text{COO}^-)_2}$	0.285928
$\beta_{\text{PZH}^+-\text{COO}^-}-\text{HCO}_3^-$	0.005264	$\beta_{\text{PZH}_2^+-\text{PZH}^+-\text{COO}^-}$	0.278674
$\beta_{\text{PZH}^+-\text{COO}^-}-\text{PZH}^+$	0.566362	$\beta_{\text{PZH}_2^+-\text{HCO}_3^-}$	0.295662
$\beta_{\text{HCO}_3^-}-\text{PZH}^+$	0.740554	$\beta_{\text{PZH}_2^+-\text{HEP}}$	0.303053
$\beta_{\text{HEP}-\text{HEPH}^+}$	0.03324	$\beta_{\text{PZH}_2^+-\text{PZ}}$	0.282362

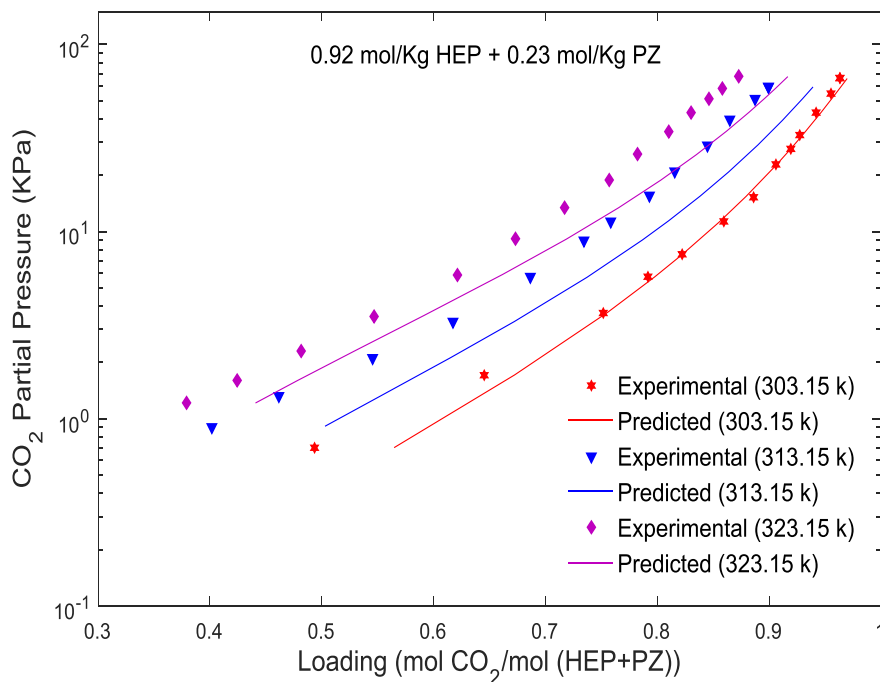


Fig. 6a. Equilibrium solubility in (CO_2 (1) + HEP (2) + PZ (3) + H_2O (4)): Experimental and model predicted CO_2 loading for (0.92 mol HEP/kg H_2O + 0.23 mol PZ/kg H_2O) blend at 303.15, 313.15 and 323.15 K.

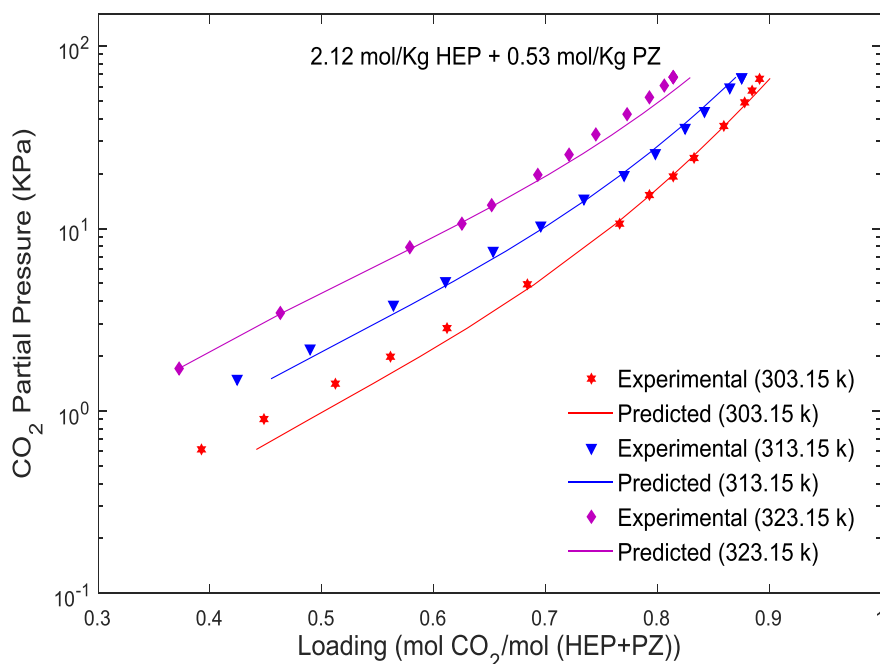


Fig. 6b. Equilibrium solubility in (CO_2 (1) + HEP (2) + PZ (3) + H_2O (4)): Experimental and model predicted CO_2 loadings for (2.12 mol HEP/kg H_2O + 0.53 mol PZ/kg H_2O) blend at 303.15, 313.15 and 323.15 K.

accept proton from the bicarbonate ion to form carbonate ion thus initially carbonate ion concentration increases up to loading 0.5. But with progression of the reaction, pH of the solution decreases and in this situation carbonate ion accept proton to form bicarbonate ion thus its concentration gradually decreases to zero. Similar concentration profile was obtained by Zhang et al. [22] through NMR studies on CO_2 absorption by tertiary alkanolamine solution.

3.5. Speciation of [CO_2 (1) + HEP (2) + PZ (3) + H_2O (4)] system

When CO_2 reacts with aqueous (HEP + PZ) blend, a number of different species are formed and exist in the liquid phase. HEP absorbs CO_2 by the formation of bicarbonate ion (HCO_3^-) and protonated amine (HEPH^+). So with increasing loading, concentration of HEPH^+ and HCO_3^- gradually increases and concentration of unreacted HEP is gradually decreased. Similar concentration profile

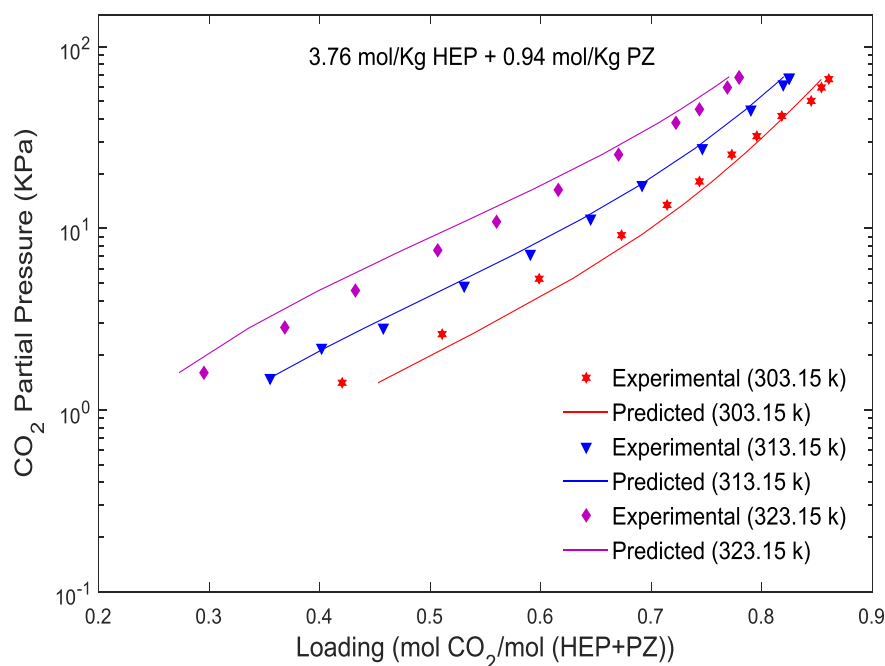


Fig. 6c. Equilibrium solubility in (CO_2 (1) + HEP (2) + PZ (3) + H_2O (4)): Experimental and model predicted CO_2 loading for (3.76 mol HEP/kg H_2O + 0.94 mol PZ/kg H_2O) blend at 303.15, 313.15 and 323.15 K.

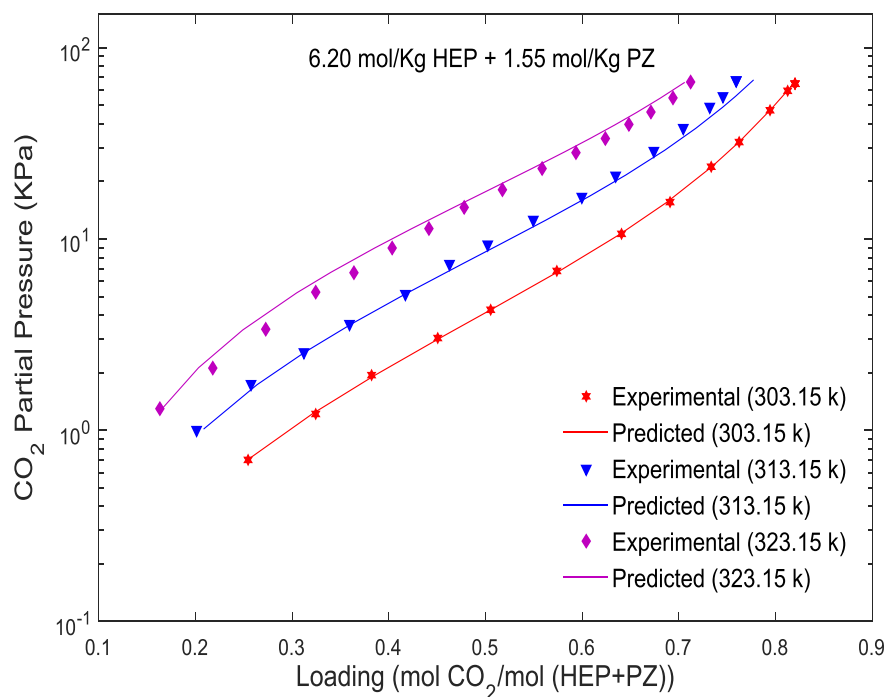


Fig. 6d. Equilibrium solubility in (CO_2 (1) + HEP (2) + PZ (3) + H_2O (4)): Experimental and model predicted CO_2 loading for (6.20 mol HEP/kg H_2O + 1.55 mol PZ/kg H_2O) blend at 303.15, 313.15 and 323.15 K.

for CO_3^{2-} ion is obtained as was obtained for single HEP solution. On the other hand, PZ absorbs CO_2 by the formation of protonated piperazine (PZH^+ and PZH_2^+), piperazine carbamate (PZCOO^-), piperazine dicarbamate ($\text{PZ}(\text{COO}^-)_2$) and protonated piperazine carbamate (PZH^+COO^-). From Fig. 8, it is found that concentration of PZCOO^- initially increases, reaches maximum and then decreases gradually with increasing loading. Initially concentration of PZH^+COO^- is increased slowly and then increased rapidly when

concentration of PZCOO^- starts to fall and then concentration of PZH^+COO^- predominates in the solution. This phenomenon can be explained by the fact that with increasing loading, pH of the solution decreases i.e. concentration of H^+ ion increases hence PZCOO^- gets protonated to form PZH^+COO^- thus concentration of PZCOO^- gradually decreases. At the start of reaction, concentration of PZ (COO^-)₂ is very low and it rises afterwards, reaches maximum then decreases; may be due to hydrolysis of dicarbamate ion with

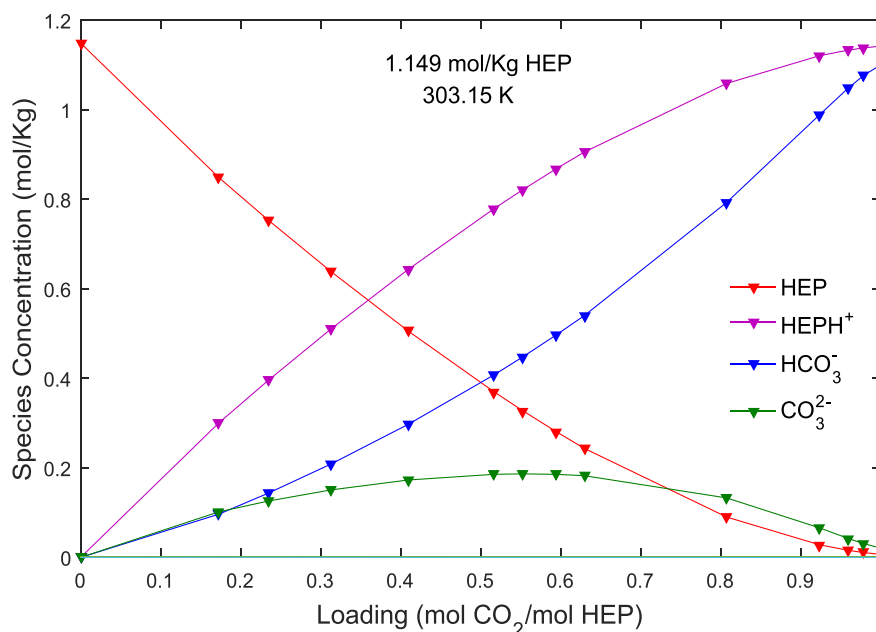


Fig. 7. Speciation plot of CO₂ loaded aqueous (1.149 mol HEP/kg H₂O) solution at 303.15 K.

increasing H⁺ ion in the solution. Concentration of PZH⁺ exists in the solution at relatively low amount but concentration of PZH₂²⁺ is negligible. Same type of concentration profiles were obtained by Kamp et al. [23], Bishnoi and Rochelle [24] for (MDEA + PZ) system using Pitzer's model and electrolyte NRTL model, respectively. Only difference in speciation between these two blends is that, in case of (MDEA + PZ) system concentration of PZH⁺ ion predominates at low loading but for (HEP + PZ) system, concentration PZCOO⁻ predominates at low loading. For (MDEA + PZ) system, PZH⁺ predominates at low loading because equilibrium constant value of protonation reaction of PZ is higher than protonation reaction of MDEA, hence, PZ has higher affinity towards H⁺ ion than MDEA and

most of the CO₂ is initially absorbed due to reaction of PZ. PZ reacts both like a base as well as nucleophile. However, for (HEP + PZ) system, equilibrium constant value of protonation reaction of PZ is lower than protonation reaction of HEP and here HEP acts like a base and PZ acts like a nucleophile. Thus, PZ helps in carbamate formation reaction and HEP helps in bicarbonate formation reaction.

3.6. Enthalpy of [CO₂ (1) + HEP (2) + H₂O (3)] system

Enthalpy of CO₂ absorption in (CO₂ (1) + HEP (2) + H₂O (3)) systems have been calculated using equations (32)–(36), set of

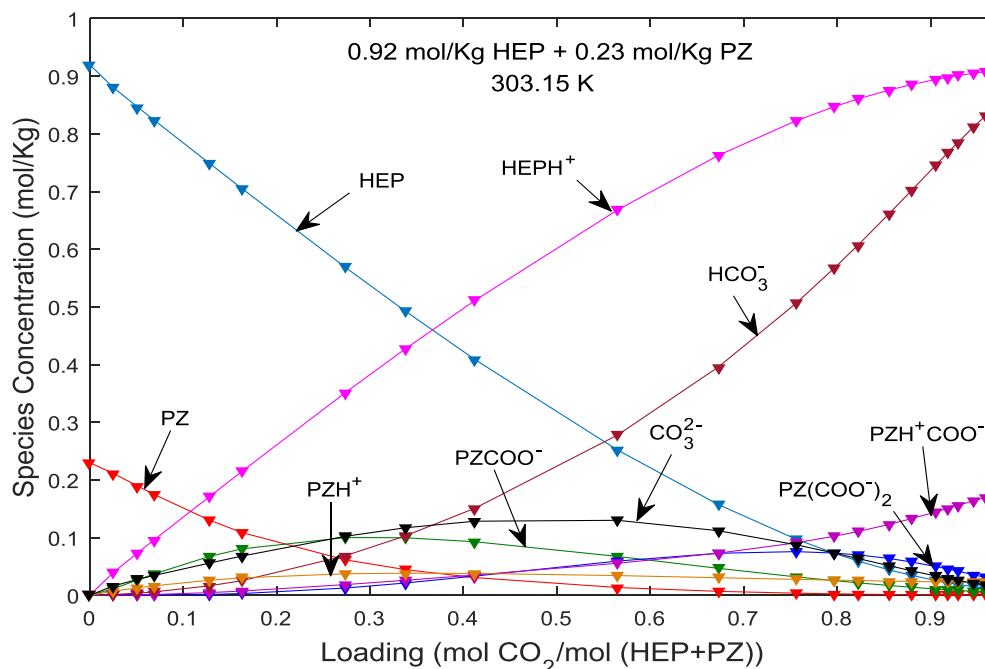


Fig. 8. Speciation plot of CO₂ loaded aqueous (0.92 mol HEP/kg H₂O + 0.23 mol PZ/kg H₂O) solution at 303.15 K.

reactions 1–4 and interaction parameters obtained by regression of the equilibrium solubility data at different temperatures and HEP concentrations. Enthalpy of solution for [HEP + CO₂+H₂O] System is the sum of enthalpy of reaction 1–4 and the enthalpy due to physical absorption of CO₂ in the amine solution. Enthalpy of solution as well as enthalpy of individual reactions are presented in Fig. 9. From Fig. 9, it is seen that enthalpy of absorption due to protonation reaction of HEP contributes maximum in the overall enthalpy (ΔH_{sol}). Enthalpy due to physical absorption (ΔH_{phy}) of CO₂ in the aqueous HEP solution has significant contribution in overall enthalpy than enthalpy (ΔH_{rxn2} and ΔH_{rxn3}) of reactions (2) and (3) respectively.

Predicted enthalpy of absorption (ΔH_{sol}) of 1.149 mol HEP/kg H₂O at three different temperatures are presented in Fig. 10. From the figure it is seen that predicted enthalpy is in the range of (80–60) KJ/mol due to CO₂ loading (0.1–1). With increasing temperature, enthalpy increases but the effect of temperature on enthalpy is not very significant here over the narrow range. Rayer and Henni [25] have experimentally produced heat of absorption for tertiary alkanolamines, 1- Dimethylamino-2-propanol (1-DMAP), 3-Dimethylamino-1-propanol (3-DMAP), N-Methyl-diethanolamine (MDEA) and they concluded that with increasing steric hindrance at amino group and increasing number of hydroxyl group (-OH) in the tertiary alkanolamine, heat of absorption decreases. Again position of the hydroxyl group with respect to amine group influences the heat of absorption. It is found that hydroxyl group present close to the amino group possesses higher enthalpy of absorption. Hence 1-DMAP has higher enthalpy of absorption than Triethanolamine (TEA) due to less number of -OH group (only one) present in the 1-DMAP molecule compared to TEA (three -OH group present in the molecule). Also 1-DMAP has higher enthalpy of absorption than 3-DMAP due to position of -OH group. In 1-DMAP, it is just two carbon apart from amine group compared to

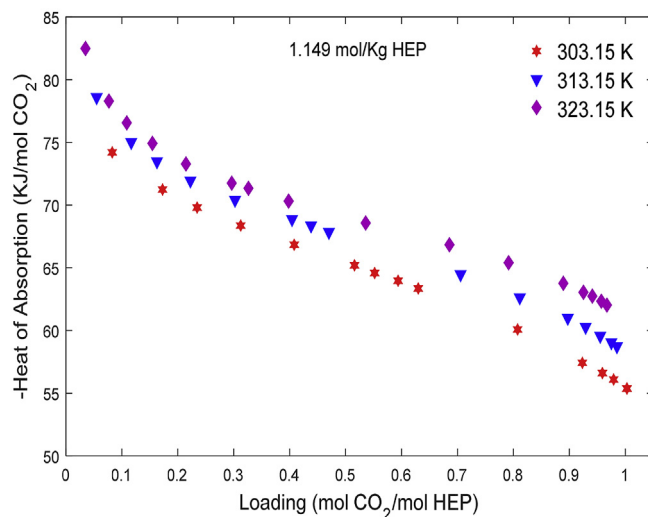


Fig. 10. Heat of absorption (ΔH_{sol} , KJ/mol CO₂) of CO₂ in (CO₂ (1) + HEP (2) + H₂O (3)) solution for (1.149 mol HEP/kg H₂O) at 303.15, 313.15 and 323.15 K.

the -OH group being three carbon apart from amine group in 3-DMAP. Hence, enthalpy of absorption order of these tertiary alkanolamines varies according to 1-DMAP > 3-DMAP > MDEA > TEA. In HEP, only one -OH group is present two carbons apart from amine group, which is similar like compound 1-DMAP. It was expected that both the compound to possess similar enthalpy of solution. According to our model prediction, enthalpy of HEP (82–55) is little lower than 1-DMAP (95–55). And this may be due to cyclic nature of HEP molecule contributing steric hindrance; unlike open chain 1-DMAP molecule.

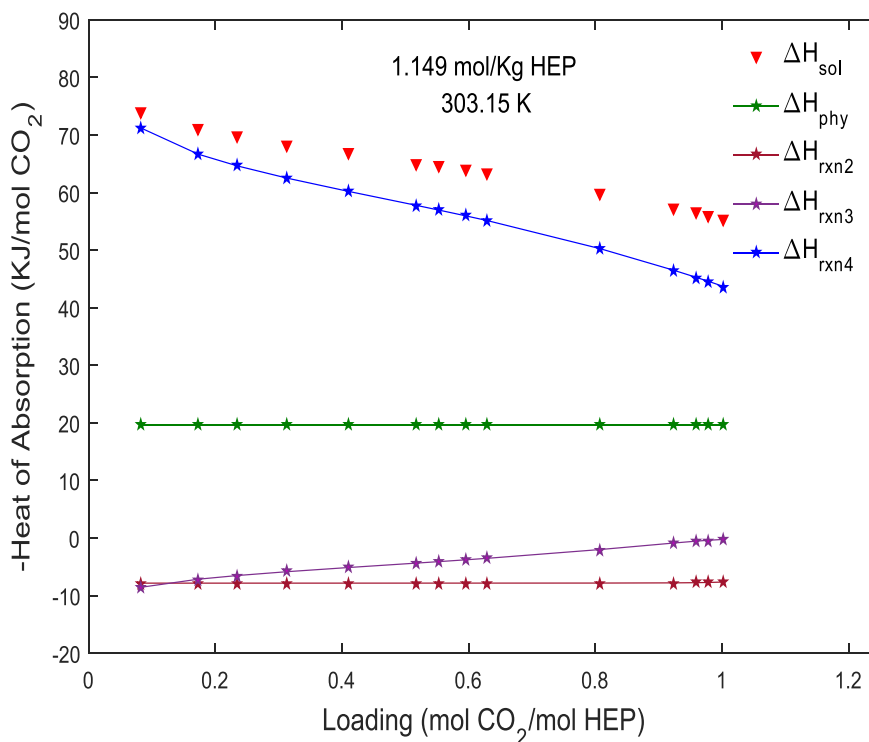
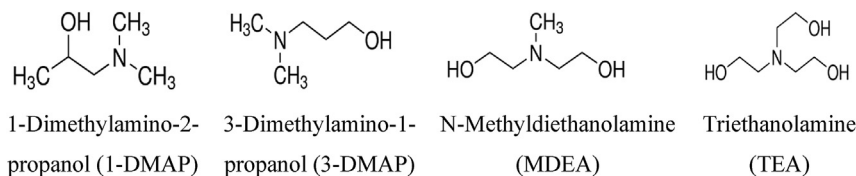


Fig. 9. Heat of absorption (KJ/mol CO₂) in aqueous (1.149 mol HEP/kg H₂O) solution with contributions from different reactions and physical absorption at 303.15 K.



3.7. Enthalpy of $[\text{CO}_2 (1) + \text{HEP} (2) + \text{PZ} (3) + \text{H}_2\text{O} (4)]$ system

Enthalpy of CO_2 absorption in $(\text{CO}_2 (1) + \text{HEP} (2) + \text{PZ} (3) + \text{H}_2\text{O} (4))$ blends were calculated using equation (32)–(36), set of

reactions 1–9 and 34 interaction parameters obtained by regression of the equilibrium solubility data at different temperatures and relative (HEP + PZ) blend compositions. Enthalpy of solution (ΔH_{sol}) for blend solution is the sum of enthalpy of reaction 1–9 and

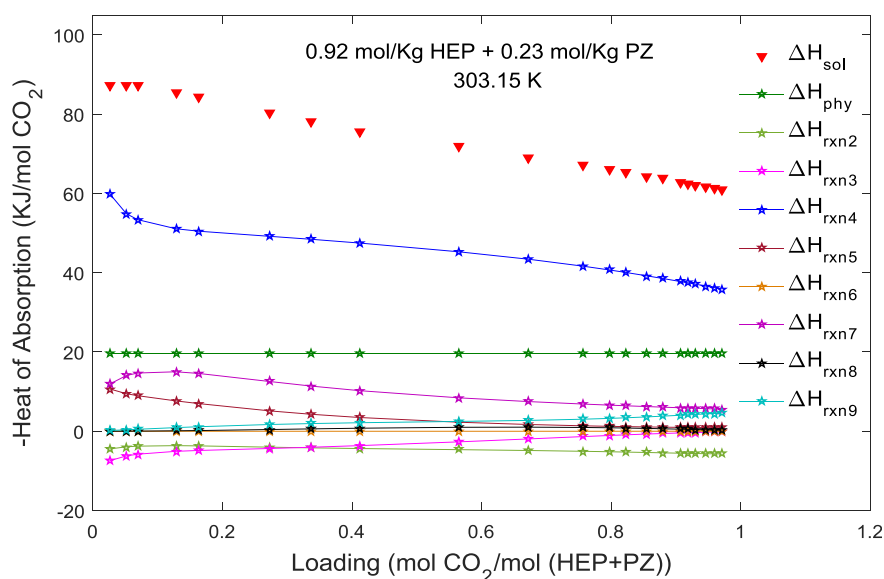


Fig. 11. Heat of absorption (ΔH_{sol} , KJ/mol CO_2) of CO_2 in $(\text{CO}_2 (1) + \text{HEP} (2) + \text{PZ} (3) + \text{H}_2\text{O} (4))$ solution for (0.92 mol HEP/kg H_2O + 0.23 mol PZ/kg H_2O) blend with contributions from different reactions and physical absorption at 303.15K.

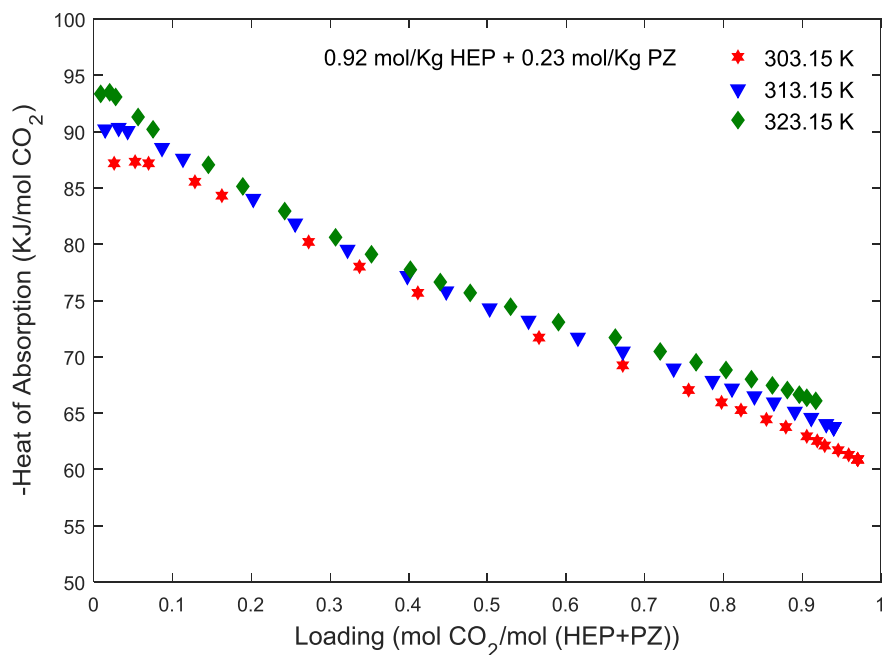


Fig. 12a. Heat of absorption (ΔH_{sol} , KJ/mol CO_2) of CO_2 in $(\text{CO}_2 (1) + \text{HEP} (2) + \text{PZ} (3) + \text{H}_2\text{O} (4))$ solution for (0.92 mol HEP/kg H_2O + 0.23 mol PZ/kg H_2O) blend at 303.15, 313.15 and 323.15 K.

enthalpy due to physical absorption (ΔH_{phy}) of CO_2 in the blend solution. Enthalpy of solution as well as enthalpy of individual reactions are presented in Fig. 11. From Fig. 11, it is seen that enthalpy of absorption due to protonation reaction of HEP contributes most

in the overall enthalpy. Enthalpies due to 1st order piperazine carbamate formation (ΔH_{rxn7}) as well as enthalpy due to protonation of piperazine (ΔH_{rxn5}) contribute in the overall enthalpy. Enthalpy due to physical absorption (ΔH_{phy}) of CO_2 in the aqueous

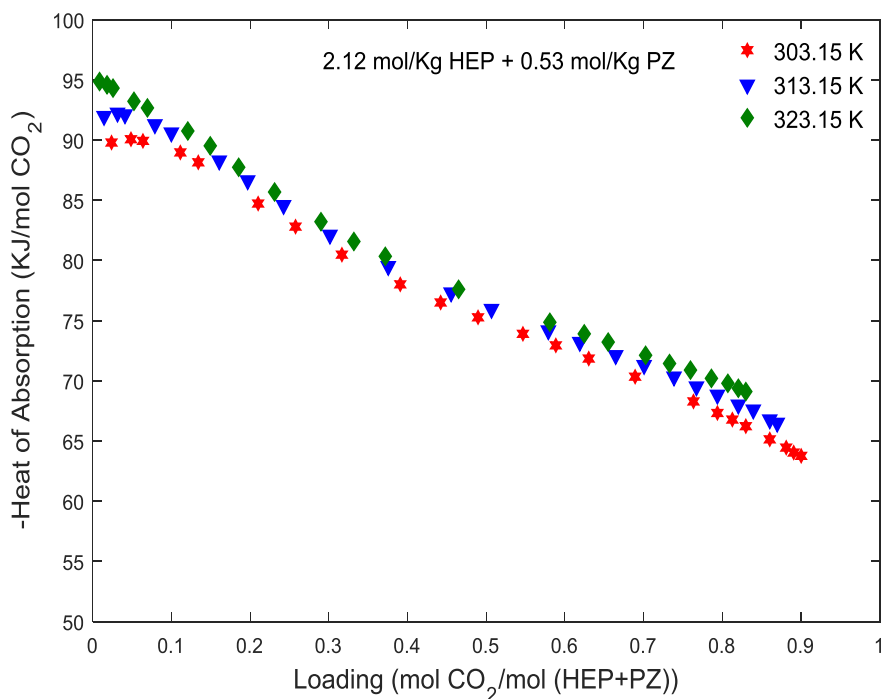


Fig. 12b. Heat of absorption (ΔH_{sol} , KJ/mol CO_2) of CO_2 in (CO_2 (1) + HEP (2) + PZ (3) + H_2O (4)) solution for (2.12 mol HEP/kg H_2O + 0.53 mol PZ/kg H_2O) blend at 303.15, 313.15 and 323.15 K.

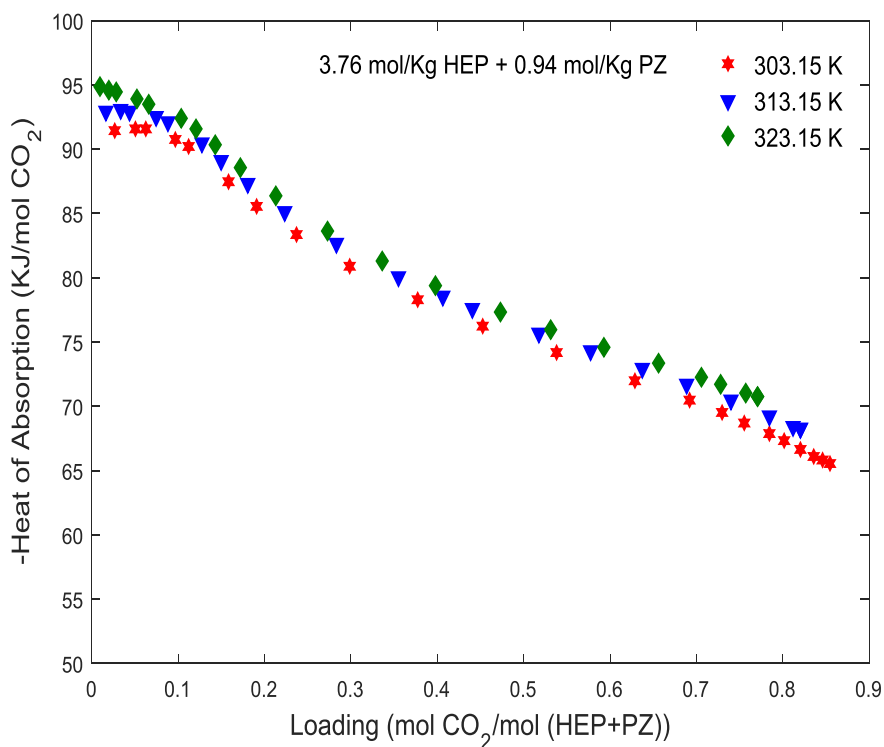


Fig. 12c. Heat of absorption (ΔH_{sol} , KJ/mol CO_2) of CO_2 in (CO_2 (1) + HEP (2) + PZ (3) + H_2O (4)) solution for (3.76 mol HEP/kg H_2O + 0.94 mol PZ/kg H_2O) blend at 303.15, 313.15 and 323.15 K.

blend solution has significant contribution in overall enthalpy over the whole spectrum of loading and rest of the reactions have negligible effect on overall enthalpy.

Predicted enthalpy of absorption for four different blends of [HEP + PZ + CO₂+H₂O] at three different temperatures is presented in Fig. 12a–d. From the figures it is seen that predicted enthalpy of solution (ΔH_{sol}) is in the range of (95–60) KJ/mol of CO₂ over the loading (0.1–1) for all the blends. With increasing temperature,

enthalpy increases but the effect of variation of temperature over this narrow range doesn't show any significant effect on enthalpy. To study the effect of blend composition on enthalpy, enthalpy of four different blends at 303.15 K has been compared and is presented in Fig. 13. It is found that with increasing total blend concentration, enthalpy increases and the effect of concentration on enthalpy is little more prominent than temperature effect. At a particular temperature, with increasing HEP concentration in the

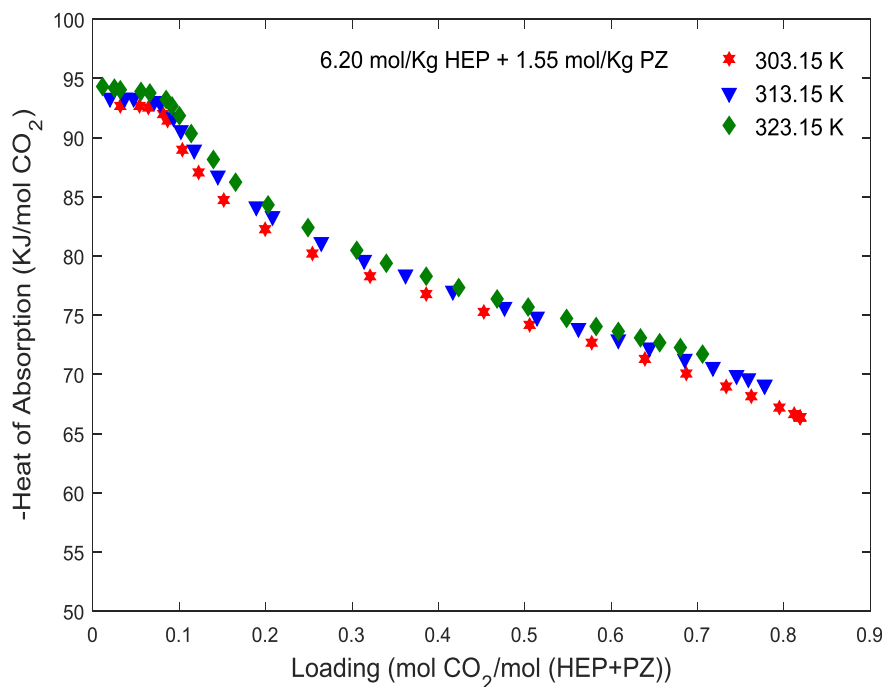


Fig. 12d. Heat of absorption (ΔH_{sol} , KJ/mol CO₂) of CO₂ in (CO₂ (1) + HEP (2) + PZ (3) + H₂O (4)) solution for (6.20 mol HEP/kg H₂O + 1.55 mol HEP/kg H₂O) blend at 303.15, 313.15 and 323.15 K.

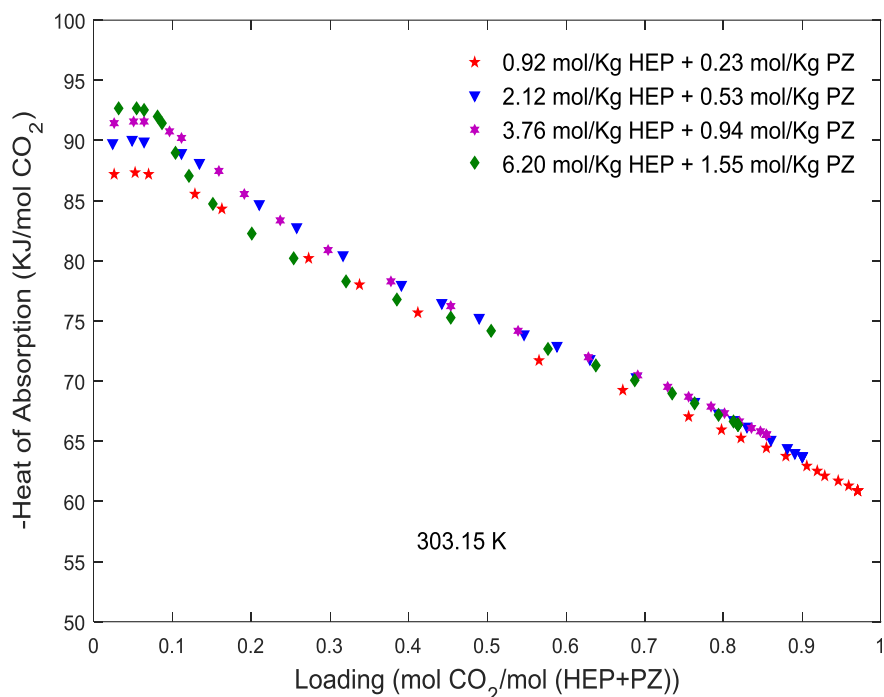


Fig. 13. Relative heat of absorptions (ΔH_{sol} , KJ/mol CO₂) of CO₂ in (CO₂ (1) + HEP (2) + PZ (3) + H₂O (4)) solutions at 303.15K.

blend, extent of protonation reaction of HEP decreases, hence the mole of CO₂ absorbed at equilibrium (As per equation (36).) decreases. And Overall enthalpy of solution, ΔH_{sol} due to CO₂ absorption in the amine solution increases.

4. Conclusions

In this article, we have studied the effectiveness of HEP solvent and its blend with piperazine towards CO₂ absorption. HEP was selected from screening experiment because of its high CO₂ absorption capacity as well as its apparent rate than industrially used MDEA. HEP, being a tertiary alkanolamine its apparent rate of CO₂ absorption is less in compared to MEA. To enhance the rate, PZ was used as a rate promoter. VLE of aqueous HEP and its blend with PZ were studied thoroughly at different temperature, pressure and relative amine concentrations. Equilibrium CO₂ solubility for both single and blended amine solutions were correlated efficiently using activity coefficient model. Model predicted speciation for both single and blended amine solutions varies with loading in accordance with the experimental and model predicted data available in the open literature. From the developed activity coefficient model enthalpy of CO₂ absorption in both single and blended solutions were estimated. Predicted enthalpy results are analysed successfully based on literature data.

Declaration of competing interest

The authors declare that they have no known competing financial interests or personal relationships that could have appeared to influence the work reported in this paper.

CRediT authorship contribution statement

Shubhashis Adak: Investigation, Writing - original draft, Software, Validation, Data curation, Formal analysis. **Madhusree Kundu:** Resources, Writing - review & editing, Visualization, Supervision, Project administration, Conceptualization.

Acknowledgement

The authors duly acknowledge the research fund provided by their institute NIT Rourkela to pursue the research.

Appendix A. Supplementary data

Supplementary data to this article can be found online at <https://doi.org/10.1016/j.fluid.2020.112463>.

References

- [1] G. Xu, C. Zhang, S. Qin, W. Gao, H. Liu, Gas-Liquid equilibrium in a CO₂-MDEA-H₂O system and the effect of piperazine on it, *Ind. Eng. Chem. Res.* 37 (1998) 1473–1477.

- [2] H. Liu, C. Zhang, G. Xu, A study on equilibrium solubility for carbon dioxide in Methyl-diethanolamine-Piperazine-Water solution, *Ind. Eng. Chem. Res.* 38 (1999) 4032–4036.
- [3] A. Kamps, J. Xia, G. Maurer, Solubility of CO₂ in (H₂O+piperazine) and in (H₂O+MDEA+piperazine), *AIChE J.* 49 (2003) 2662–2670.
- [4] W. Böttinger, M. Maiwald, H. Hasse, Online NMR spectroscopic study of species distribution in MDEA-H₂O-CO₂ and MDEA-PIP-H₂O-CO₂, *Ind. Eng. Chem. Res.* 47 (2008) 7917–7926.
- [5] D. Speyer, V. Ermatchkov, G. Versteeg, Solubility of carbon dioxide in aqueous solutions of N-methyl-diethanolamine and piperazine in the low gas loading region, *J. Chem. Eng. Data* 55 (2010) 283–290.
- [6] P. Derks, J. Hogendoorn, G. Versteeg, Experimental and theoretical study of the solubility of carbon dioxide in aqueous blends of piperazine and N-methyl-diethanolamine, *J. Chem. Thermodyn.* 42 (2010) 151–163.
- [7] H. Svensson, C. Hultberg, H. Karlsson, Heat of absorption of CO₂ in aqueous solutions of N-methyl-diethanolamine and piperazine, *Int. J. Greenh. Gas Contr.* 17 (2013) 89–98.
- [8] J. Huang, M. Gong, X. Dong, X. Li, J. Wu, CO₂ solubility in aqueous solutions of N-methyl-diethanolamine+piperazine by electrolyte NRTL model, *Sci. China Chem.* 59 (2015) 360–369.
- [9] S. Adak, M. Kundu, Vapor-liquid equilibrium and physicochemical properties of novel aqueous blends of (2-diethylaminoethanol + piperazine) for CO₂ appropriation, *J. Chem. Eng. Data* 62 (2017) 1937–1947.
- [10] R. Ramezani, S. Mazinani, R. Di Felice, S. Darvishmanesh, B. Van der Bruggen, Selection of blended absorbents for CO₂ capture from flue gas: CO₂ solubility, corrosion and absorption rate, *Int. J. Greenh. Gas Contr.* 62 (2017) 61–68.
- [11] Y. Du, Amine Solvent Development for Carbon Dioxide Capture, Ph. D. The University of Texas at Austin, 2016.
- [12] F. Chowdhury, H. Yamada, T. Higashii, K. Goto, M. Onoda, CO₂ capture by tertiary amine absorbents: a performance comparison study, *Ind. Eng. Chem. Res.* 52 (2013) 8323–8331.
- [13] M. Xiao, W. Zheng, H. Liu, P. Tontiwachwuthikul, Z. Liang, Analysis of equilibrium CO₂ solubility and thermodynamic models for aqueous 1-(2-hydroxyethyl)-piperidine solution, *AIChE J.* 65 (2019), e16605.
- [14] S. Bishnoi, G. Rochelle, Absorption of carbon dioxide into aqueous piperazine: reaction kinetics, mass transfer and solubility, *Chem. Eng. Sci.* 55 (2000) 5531–5543.
- [15] M. Park, O. Sandall, Solubility of carbon dioxide and nitrous oxide in 50 mass methyl-diethanolamine, *J. Chem. Eng. Data* 46 (2001) 166–168.
- [16] T. Edwards, G. Maurer, J. Newman, J. Prausnitz, Vapor-liquid equilibria in multicomponent aqueous solutions of volatile weak electrolytes, *AIChE J.* 24 (1978) 966–976.
- [17] H. Hetzer, R. Robinson, R. Bates, Dissociation constants of piperazinium ion and related thermodynamic quantities from 0 to 50°, *J. Phys. Chem.* 72 (1968) 2081–2086.
- [18] V. Ermatchkov, A. Pérez-Salado Kamps, G. Maurer, Chemical equilibrium constants for the formation of carbamates in (carbon dioxide+piperazine+water) from -NMR-spectroscopy, *J. Chem. Thermodyn.* 35 (2003) 1277–1289.
- [19] E. Guggenheim, R. Stokes, Activity coefficients of 2 : 1 and 1 : 2 electrolytes in aqueous solution from isopiestic data, *Trans. Faraday Soc.* 54 (1958) 1646.
- [20] K. Pitzer, L. Silvester, Thermodynamics of electrolytes. VI. Weak electrolytes including H₃PO₄, *J. Solut. Chem.* 5 (1976) 269–278.
- [21] S. Xu, F. Otto, A. Mather, Dissociation constants of some alkanolamines, *Can. J. Chem.* 71 (1993) 1048–1050.
- [22] R. Zhang, Z. Liang, H. Liu, W. Rongwong, X. Luo, R. Idem, et al., Study of formation of bicarbonate ions in CO₂-loaded aqueous single 1DMA2P and MDEA tertiary amines and blended MEA-1DMA2P and MEA-MDEA amines for low heat of regeneration, *Ind. Eng. Chem. Res.* 55 (2016) 3710–3717.
- [23] A. Kamps, J. Xia, G. Maurer, Solubility of CO₂ in (H₂O+piperazine) and in (H₂O+MDEA+piperazine), *AIChE J.* 49 (2003) 2662–2670.
- [24] S. Bishnoi, G. Rochelle, Thermodynamics of piperazine/methyl-diethanolamine/water/carbon dioxide, *Ind. Eng. Chem. Res.* 41 (2002) 604–612.
- [25] A. Rayer, A. Henni, Heats of absorption of CO₂ in aqueous solutions of tertiary amines: N-methyl-diethanolamine, 3-Dimethylamino-1-propanol, and 1-Dimethylamino-2-propanol, *Ind. Eng. Chem. Res.* 53 (2014) 4953–4965.